Int. J. Devl Neuroscience xxx (2011) xxx–xxx

Contents lists available at ScienceDirect

International Journal of Developmental Neuroscience

journal homepage: www.elsevier.com/locate/ijdevneu

Hypertrophy and neuron loss: structural changes in sheep SCG induced by unilateral sympathectomy

Emerson T. Fioretto[a], Sheila C. Rahal[b], Alexandre S. Borges[c], Terry M. Mayhew[d], Jens R. Nyengaard[e], Julio S. Marcondes[c], Júlio C. de Carvalho Balieiro[f], Carlos R. Teixeira[b], Mariana P. de Melo[g], Fernando V. Lobo Ladd[h], Aliny A.B. Lobo Ladd[h], Ana R. de Lima[i], Andrea A.P. da Silva[h], Antonio A. Coppi[h,*]

[a] Department of Morphology, Center for Biological and Health Sciences, Laboratory of Cellular and Structural Biology, Federal University of Sergipe (UFS), Aracaju, Brazil
[b] School of Veterinary Medicine and Animal Science, UNESP - Univ Estadual Paulista, Campus, Botucatu, Department of Veterinary Surgery and Anesthesiology, Brazil
[c] School of Veterinary Medicine and Animal Science, UNESP - Univ Estadual Paulista, Campus, Botucatu, Department of Veterinary Clinics, Brazil
[d] School of Biomedical Sciences, Queen's Medical Centre, University of Nottingham, Nottingham NG7 2UH, United Kingdom
[e] Stereology and Electron Microscopy Laboratory, Centre for Stochastic Geometry and Advanced Bioimaging, Aarhus University Hospital, Aarhus, Denmark
[f] Department of Basic Science, College of Food Engineering and Animal Science, University of São Paulo (USP), Pirassununga, Brazil
[g] Department of Statistics, Institute of Mathematics and Statistics, University of São Paulo, Brazil
[h] Laboratory of Stochastic Stereology and Chemical Anatomy (LSSCA), Department of Surgery, College of Veterinary Medicine, University of São Paulo (USP), São Paulo, Brazil
[i] Department of Surgery, College of Veterinary Medicine, University of São Paulo (USP), São Paulo, Brazil

ARTICLE INFO

Article history:
Received 6 February 2011
Accepted 7 February 2011

Keywords:
Superior cervical ganglionectomy
Stereology
SCG
Sheep

ABSTRACT

Recently, superior cervical ganglionectomy has been performed to investigate a variety of scientific topics from regulation of intraocular pressure to suppression of lingual tumour growth. Despite these recent advances in our understanding of the functional mechanisms underlying superior cervical ganglion (SCG) growth and development after surgical ablation, there still exists a need for information concerning the quantitative nature of the relationships between the removed SCG and its remaining contralateral ganglion and between the remaining SCG and its modified innervation territory. To this end, using design-based stereological methods, we have investigated the structural changes induced by unilateral ganglionectomy in sheep at three distinct timepoints (2, 7 and 12 weeks) after surgery. The effects of time, and lateral (left-right) differences, were examined by two-way analyses of variance and paired *t*-tests. Following removal of the left SCG, the main findings were: (i) the remaining right SCG was bigger at shorter survival times, i.e. 74% at 2 weeks, 55% at 7 weeks and no increase by 12 weeks, (ii) by 7 weeks after surgery, the right SCG contained fewer neurons (no decrease at 2 weeks, 6% fewer by 7 weeks and 17% fewer by 12 weeks) and (iii) by 7 weeks, right SCG neurons were also larger and the magnitude of this increase grew substantially with time (no rise at 2 weeks, 77% by 7 weeks and 215% by 12 weeks). Interaction effects between time and ganglionectomy-induced changes were significant for SCG volume and mean perikaryal volume. These findings show that unilateral superior cervical ganglionectomy has profound effects on the contralateral ganglion. For future investigations, it would be interesting to examine the interaction between SCGs and their innervation targets after ganglionectomy. Is the ganglionectomy-induced imbalance between the sizes of innervation territories the milieu in which morphoquantitative changes, particularly changes in perikaryal volume and neuron number, occur? Mechanistically, how would those changes arise? Are there any grounds for believing in a ganglionectomy-triggered SCG cross-innervation and neuroplasticity?

1. Introduction

The superior cervical ganglion (SCG), which is a paravertebral ganglion, provides sympathetic input to the head and neck as well as to the mandible, submandibular glands, pineal and cerebral vessels (Andrews, 1996; Steele et al., 2006). In addition, SCG plays an important role in some neuropathies including Horner's syndrome (Kisch, 1991; Boydell, 1995; Bell et al., 2001).

* Corresponding author at: Departamento de Cirurgia, Faculdade de Medicina Veterinária e Zootecnia, Universidade de São Paulo, Av. Prof. Dr. Orlando Marques de Paiva, 87, CEP 05508-270, São Paulo, SP, Brazil. Tel.: +55 11 3091 1214; fax: +55 11 3091 1214.
E-mail address: guto@usp.br (A.A. Coppi).

0736-5748/$36.00 © 2011 ISDN. Published by Elsevier Ltd. All rights reserved.
doi:10.1016/j.ijdevneu.2011.02.002

Superior cervical ganglionectomy (SCGx) has been performed to investigate a wide variety of scientific topics including regulation of intraocular pressure (Zhan et al., 1999), secretion of the pineal hormone melatonin (Karasek et al., 2002), the relationship between periodontal disease and sympathetic nervous system-related bone remodelling (Kim et al., 2009) and suppression of tumour growth in cancer of the rat tongue (Raju et al., 2009). Despite these advances in our understanding of the functional mechanisms underlying SCG growth and development after unilateral or bilateral surgical ablation, there is still a lack of three-dimensional stereological morphoquantitative information about the nature of relationships between the removed SCG and its remaining contralateral ganglion and between the remaining SCG and its resulting broader and imbalanced innervation territory.

By employing two-dimensional model-based morphometric procedures, Usui and Sakamaki (1998) reported on the effect of a unilateral SCGx on the contralateral ganglion neurons of Sprague–Dawley rats. However, the aforementioned authors did not use design-based methods to derive three-dimensional structural data, and their results are therefore questionable since the neuron profile cross-sectional area and neuron profile density were assumed to be the true cell size and the true total number of cells, respectively, which confirms the danger of drawing conclusions based only upon ratios without considering the reference space – the so-called 'reference trap' – (Braendgaard and Gundersen, 1986; Hunziker and Cruz-Orive, 1986; Cruz-Orive, 1994; Mayhew, 2008).

In the light of these uncertainties, we decided to embark on a light-microscopic study of unilateral ganglionectomy-induced structural changes in the developing sheep SCG at three distinct timepoints after surgery (2, 7 and 12 weeks) using 3D design-based stereological methods. The data raised in this study provide a structural foundation which is novel and important for explaining the processes underlying SCG adaptation and remodelling after unilateral ganglionectomy. We hope that the results obtained by this work will pave the way for translational studies and extend the basic-research knowledge to clinicians and surgeons devoted to understanding the autonomic nervous system of large mammals in the context of veterinary medicine.

2. Materials and methods

2.1. Animals

The present study was approved by the Animal Care Committee of the College of Veterinary Medicine of the University of São Paulo. Left and right SCGs were obtained from $n = 15$ male sheep (Santa Inês breed) maintained in the Department of Veterinary Surgery and Anaesthesiology, School of Veterinary Medicine and Animal Science in Botucatu, São Paulo, Brazil. Animals were pre-pubertal (Wańkowska and Polkowska, 2006; Wańkowska et al., 2008a,b; Polkowska et al., 2008), i.e. 4 months old, and the mean (standard deviation) body weight was 15 kg (2 kg). According to the period of examination, animals were divided into three groups which were evaluated 2 weeks (group 2wk), 7 weeks (group 7wk) and 12 weeks (group 12wk) after surgery.

An age-matched sham-control group was not added to the present study design for two reasons: (i) a plethora of in-depth and large-scale studies on the effects of postnatal development – maturation and ageing – on SCG structure in various species: rats, guinea pigs, pacas, capybaras, horses, cats and dogs (Ribeiro et al., 2004; Ribeiro, 2006; Melo et al., 2009; Abrahão et al., 2009; Toscano et al., 2009). These studies have clearly shown no differences in structure (ganglion volume, neuron size and neuron number) between 4- and 7-month-old subjects; (ii) all sheep used in this study were in the same pre-pubertal phase of development, which ranges from 15 weeks to 30 weeks after birth (Wańkowska and Polkowska, 2006; Wańkowska et al., 2008a,b; Polkowska et al., 2008).

2.2. Operative technique

Animals were sedated with a 0.1 mg/kg i.m. injection of acepromazine (Bayer S.A. São Paulo, Brazil) and 0.3 mg/kg butorphanol tartrate (Bayer). Anaesthesia involved a combination of a 20 mg/kg i.m. injection of ketamine chloride (Bayer) and 1.5 mg/kg xylazine hydrochloride (Bayer) and was maintained with 0.85–0.95% halothane. The surgical procedure was slightly modified from that described elsewhere (Appleton and Waites, 1957). Animals were placed in the right lateral decubitus position, with head and neck wholly extended. A ventro-lateral approach was adopted with a skin incision from the proximal portion of the mandible towards the external base of the auricle. On the superficial surgical plane, the following constituent parts were identified: left external jugular vein, left parotid gland and adipose tissue. The vagosympathetic trunk, common carotid artery and internal jugular vein were identified on the deeper surgical plane. All important cervical structures were retracted down to the level of the jugulohyoideus muscle which was sectioned to allow for removal of the left SCG. After removal, the thickness, width and length of the left SCG were measured using a digital pachymeter (Digimess Instrumentos de Precisão Ltda, São Paulo, Brazil) and immersion-fixed with 5% glutaraldehyde and 1% formaldehyde in sodium cacodylate buffer (0.1 M, pH 7.4).

The surgical intervention was accomplished by suturing the ends of the jugulohyoideus muscle as well as subcutaneous tissue and the skin. The retracted muscles and subcutaneous tissue were sutured using cruciate mattress and simple continuous methods respectively. All suturing was performed using a monofilament-nylon thread. Post-operative antibiotic therapy comprised 3 days of 20 mg/kg i.m. benzathine ampicillin (Schering-Plough Animal Health, Cotia, São Paulo, Brazil). Flunixin meglumine (1.1 mg/kg i.m., Schering-Plough Animal Health) and sodium dipyrone (5 ml i.m., Schering-Plough Animal Health) were administered for 3 days. After surgery, animals were kept in 6 m^2 pens for clinical examination.

2.3. Clinical examination

Animals were examined during the three post-operative timepoints. The following clinical parameters were investigated: temperature of face and ear by thermographic analysis (Purohit et al., 1980), ptosis, miosis and sudoresis.

2.4. Euthanasia and histology

At each timepoint, sheep were euthanised using a 200 mg/kg i.v. dose of pentobarbitone. Next, a bulbed cannula was inserted into the left ventricle of the heart and a cleaning solution of 0.1 M, pH 7.4 phosphate-buffered saline (PBS) (Sigma–Aldrich, São Paulo, Brazil) containing 2% heparin (Roche-Brasil, São Paulo, Brazil) and 0.1% sodium nitrite (Sigma–Aldrich) was injected via the ascending aorta. This was followed by perfusion-fixation with 5% glutaraldehyde and 1% formaldehyde in sodium cacodylate buffer (0.1 M, pH 7.4). The right SCGs were dissected out and their wet weights were converted into volumes using a tissue density of 1.06 g cm^{-3} (Weibel, 1979) for estimating tissue shrinkage distortion. The thickness, width and length of each right SCG were also measured using a digital pachymeter (Digimess).

2.5. Embedding procedures

In order to produce vertical and uniform random (VUR) sections (Baddeley et al., 1986; Tandrup, 1993; Tandrup and Braendgaard, 1994), SCGs were rotated along their own long axis using a bar rotator and their vertical axes were marked using a Tissue Marking Dye System (Cancer Diagnostics, Inc. Birmingham, USA). Subsequently, left and right SCGs were washed in sodium cacodylate buffer, post-fixed in a buffered solution of 2% osmium tetroxide, stained en bloc with a saturated aqueous solution of uranyl acetate (Electron Microscopy Sciences (EMS), Hatfield, PA, USA) dehydrated in graded ethanol concentrations and propylene oxide (EMS) and embedded in Araldite 502 (EMS). Araldite blocks of tissue were polymerised in the oven at 60–70 °C for three days. For light microscopy, 2- and 0.5-μm thick VUR sections were exhaustively cut with glass knives using a UC6 automatically calibrated Leica ultramicrotome (for more details, see Section 2.6.2). Next, sections were collected onto glass slides, dried on a hot plate, stained with toluidine blue and mounted under a coverslip with a drop of Araldite. Section images were acquired using a DMR Leica microscope (Leica Microsystems, Wetzlar, Germany) equipped with a High-End DP 72 Olympus digital camera (Olympus, Essex, United Kingdom) and projected onto a computer monitor. Stereological analyses were performed using the auto-disector and the nucleator procedure of the newCAST Visiopharm stereology system version 3.4.1.0 (Visiopharm, Copenhagen, Denmark).

2.6. Design-based stereology

2.6.1. Volume of ganglion, V_{SCG}

The total volume of each SCG was estimated by means of the Cavalieri principle (Gundersen and Jensen, 1987; Gundersen et al., 1999) in the same reference sections used for disectors. Briefly, SCG tissue blocks were exhaustively serially sectioned and every 250th section was sampled and measured for cross-sectional area. Then:

$$V_{SCG} := T \cdot \Sigma A_{SCG}$$

where T is the between-section distance (500 μm) and ΣA_{SCG} is the sum of the delineated profile areas of the chosen set of SCG sections. The between-section distance was determined by cutting 40 sets of sections each set having a distance of 12.5 μm (a 2-μm thick section followed by another 0.5-μm thick section and by six more 2-μm thick sections). Profile areas were estimated from the numbers of randomly positioned test points (~200 per SCG) hitting the whole reference space and the areal equivalent of a test point. Irrespective of groups, the mean volume shrinkage (coefficient of variation, CV, expressed as a decimal fraction of the mean) was

Please cite this article in press as: Fioretto, E.T., et al., Hypertrophy and neuron loss: structural changes in sheep SCG induced by unilateral sympathectomy. Int. J. Dev. Neurosci. (2011), doi:10.1016/j.ijdevneu.2011.02.002

estimated to be 3.8% (0.21) for the left SCG and 3.6% (0.20) for the right SCG. No correction for global shrinkage was performed since the between-side SCG difference was not significant.

2.6.2. Total number of neurons, N_{SCG}

The physical fractionator was used for estimating the total number of SCG neurons (Gundersen, 1986; Mayhew, 1991). Each Araldite block was exhaustively serially sectioned into 2- and 0.5-μm thick sections and a sampling fraction (ssf, 1/250) of these 'reference' sections was selected together with two companion 'look-up' sections, which were 0.5 μm (look-up 1 section) and 12.5 μm (look-up 2 section) distant from the reference sections. Look-up 1 sections were used for sampling the nucleolus and estimating neuron volume. Look-up 2 sections were used for sampling the perikaryon (soma) and estimating the total number of neurons. The disector height was 12.5 μm. An area sampling fraction (asf) of 1/7 (group 2wk) or 1/9 (groups 7wk and 12wk) of the chosen SCG sections was sampled using 2D unbiased counting frames with a frame area equivalent to 29,900 μm^2 (Gundersen, 1977). The same sampled area was followed towards eight consecutive sections, i.e. one 2-μm thick section followed by another 0.5-μm thick section and six more 2-μm thick sections.

For group 2wk, an average of 246 disectors was used to count 158 neurons (ΣQ^-). In group 7wk, 136 disectors were applied to count 162 neurons. In group 12wk, 270 disectors were employed to count 155 neurons. The total number of SCG neurons was then estimated by multiplying the counted number of particles by the reciprocal of sampling fractions:

$$N_{SCG} := \mathrm{ssf}^{-1} \cdot \mathrm{asf}^{-1} \cdot \Sigma Q^-$$

where ssf is the section sampling fraction, asf is the area sampling fraction and ΣQ^- is the total number of particles counted using physical disectors.

2.6.3. Mean volume of SCG neuron, $\bar{v}_{N\,SCG}$

The mean perikaryal volume of SCG neurons was estimated by the nucleator method (Gundersen, 1988) using the 4 half-line nucleator probe available in the newCAST Visiopharm stereology system and in the same reference sections used for total number estimation. Nucleoli were sampled using one 2-μm and one 0.5-μm thick section in a physical disector. The following formula was used to estimate the mean perikaryal volume:

$$\bar{v}_{N\,SCG} := \Sigma \left(\frac{4\pi}{3} \right) \bar{l}_n^3$$

where $\bar{l}_n^3$ is the mean of all cubed distances from a central point (nucleolus) within the perikaryon to its cell boundaries.

2.7. Statistical analyses

The precision of a stereological estimate was expressed as a coefficient of error (CE) calculated as described by Gundersen et al. (1999). Stereological data were expressed as group mean (observed coefficient of variation, CV_{obs}) where CV_{obs} represents standard deviation/mean. Group differences were assessed by analysis of variance (ANOVA) and paired *t*-tests using Minitab version 15 and Unistat version 5.5 statistical software. With two-way ANOVA, we examined the main effects of post-operative time and ganglionectomy-induced changes. The interaction term generated by this test identifies whether or not the main effects act independently, synergistically or antagonistically. In recognition that left and right SCGs came from the same animals, lateral differences were analysed further by paired *t*-tests. Null hypotheses (no main or interaction effects) were rejected when the probability level for apparent differences was $p < 0.05$.

3. Results

3.1. Clinical findings

During surgical intervention, a rise in the temperature of the left ear and left side of the face was observed in all animals. Post-operatively, the main clinical findings were [a] an increase in the temperature of the ear and face (Fig. 1), [b] ptosis of the upper eyelid, [c] miosis and [d] absence of sudoresis which occurred in the same (left) side from which the SCG was removed. The increase in ear temperature was a persistent clinical symptom from the first to the second week (group 2wk), between weeks 1 and 7 (group 7wk) and until week 8 after surgery (group 12wk). In all groups, the rise in face temperature was discrete and persisted for 2 weeks after surgery. Furthermore, miosis of the left eye occurred in the animals from all groups and lasted 2 weeks after surgery and the absence of sudoresis on the left side of the nasal plane persisted for 2 weeks (groups 2wk and 12wk) and lasted 4 weeks in the animals from group 7wk. Finally, ptosis of the left upper eyelid occurred at 2, 7 and 12 weeks.

Fig. 1. Thermographic analysis of the face temperature of a sheep after left SCG ganglionectomy. Note the rise in the temperature of the left side of the face (yellow areas labelled with *) 2 h after the surgical procedure. Also observe areas with increased temperature (red areas) on the left ear and on the left side of the nasal plane. (For interpretation of the references to color in this figure legend, the reader is referred to the web version of the article.)

3.2. SCG structure

In all animals, irrespective of groups and side of the body, the left and right SCGs were roughly spindle-shaped and located in the most cranial part of the neck. Dorsally, ganglia were in contact with the vagus nerve and, ventrally, they were close to the occipital artery. The caudal pole of SCG continued into the cervical sympathetic trunk.

In group 2wk, left SCG width, length and thickness were 3.2 mm (0.27), 5.6 mm (0.26) and 2.6 mm (0.21), respectively. For the right SCG, width, length and thickness were 4.3 mm (0.17), 8.6 mm (0.16) and 2.9 mm (0.23), respectively. For group 7wk, left SCG width, length and thickness were 4.2 mm (0.26), 6.1 mm (0.12) and 2.7 mm (0.20), respectively. The right SCG, width, length and thickness were 4.2 mm (0.17), 7.7 mm (0.26) and 2.9 mm (0.14), respectively. In group 12wk, left SCG width, length and thickness were 4.4 mm (0.17), 7.1 mm (0.16) and 2.4 mm (0.23), whilst the same figures in the right SCG were 3.5 mm (0.21), 7.3 mm (0.13) and 2.4 mm (0.13) respectively. Apparent differences in linear dimensions between post-operative times and between right and left SCGs were not significant, for either ganglion width ($p = 0.13$) and length ($p = 0.15$) or ganglion thickness ($p = 0.22$).

Regardless of body side, SCG comprised clusters of neurons separated by nerve fibres, blood vessels and prominent septa of connective tissue. Ganglion neuron profiles were roughly circular or oval in shape. In the left SCG (collected during surgery), neurons were packed and homogeneously distributed. However, in the right SCG (harvested 2, 7 and 12 weeks after surgery) neurons were larger, not homogeneously distributed, further apart and separated by spaces mainly occupied by neuropil (neurites and glial cells) and by blood vessels and connective tissue. Irrespective of body side and post-operative period, neuron nuclei were located either centrally or eccentrically in the perikarya (Fig. 2A–F).

Please cite this article in press as: Fioretto, E.T., et al., Hypertrophy and neuron loss: structural changes in sheep SCG induced by unilateral sympathectomy. Int. J. Dev. Neurosci. (2011), doi:10.1016/j.ijdevneu.2011.02.002

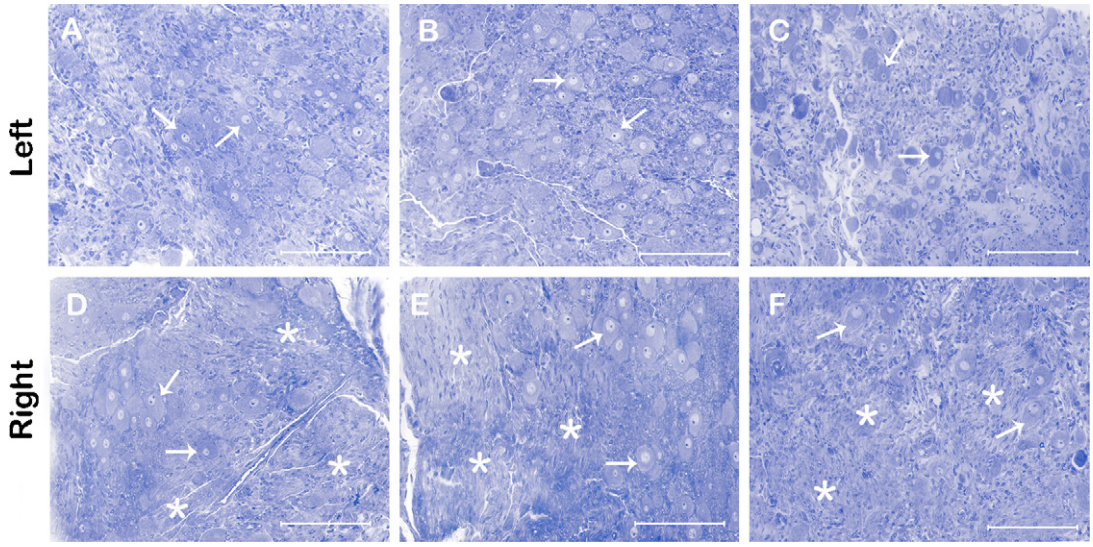

Fig. 2. Light-microscopic images of toluidine blue-stained, 2-μm thick, semithin resin sections of left (excised) and right (remaining) sheep SCGs from groups 2wk (A and D), 7wk (B and E) and 12wk (C and F) post-surgery. Note the densely packed and homogeneously distributed smaller neurons (arrows in A–C) and the larger neurons non-uniformly distributed (arrows in D–F) and separated by spaces mainly occupied by neuropil (neurites and glial cells) and by blood vessels and connective tissue (*). Scale bar = 200 μm.

3.3. Stereological data

3.3.1. Volume of ganglion, V_{SCG}

SCG volumes are summarised in Fig. 3. For group 2wk, the volumes of left and right SCGs were 43.0 mm^3 (0.22) and 74.7 mm^3 (0.09) respectively. In group 7wk, the volumes of left and right SCGs were 45.7 mm^3 (0.15) and 70.7 mm^3 (0.22) respectively. The corresponding values in group 12wk were 39.2 mm^3 (0.15) and 48.8 mm^3 (0.09). Two-way ANOVA demonstrated significant main effects of post-operative time ($p = 0.001$) and ganglionectomy-induced changes ($p < 0.001$) together with a significant post-operative time × ganglionectomy-induced changes interaction effect ($p = 0.029$). The right SCG was always bigger than the left SCG irrespective of the week studied but the magnitude of these differences diminished with time after surgery. Paired tests confirmed that ganglionectomy-induced differences were significant at 2 weeks ($p < 0.001$) and 7 weeks ($p = 0.004$) but not at 12 weeks. The precision of estimated left SCG volume (expressed as CE) was 0.05 for group 2wk, 0.08 for group 7wk and 0.06 for group 12wk. For the right SCG, the values were 0.05, 0.06 and 0.06 for groups 2wk, 7wk and 12wk, respectively.

3.3.2. Total number of neurons, N_{SCG}

In group 2wk (see Fig. 4), total numbers of neurons per left and right SCG were 265,100 (0.24) and 249,900 (0.18), respectively. For other groups, corresponding numbers were 358,700 (0.24) and 335,600 (0.27) for group 7wk and 416,000 (0.14) and 344,000 (0.07) for group 12wk. SCGs in the latter group had more neurons than those in groups 2wk and 7wk. With two-way ANOVA, this post-operative time effect was highly significant ($p = 0.001$) but no significant ganglionectomy-induced or interaction effects were detected. However, paired *t*-tests showed that numbers were not significantly different between left and right SCGs in group 2wk but were greater in left SCGs at 7 ($p = 0.034$) and 12 weeks ($p = 0.018$) post surgery. For the left SCG, the precision of estimated N_{SCG} was 0.05 for group 2wk, 0.06 for group 7wk and 0.05 for group 12wk. For the right SCG, the corresponding values were 0.04, 0.06 and 0.05.

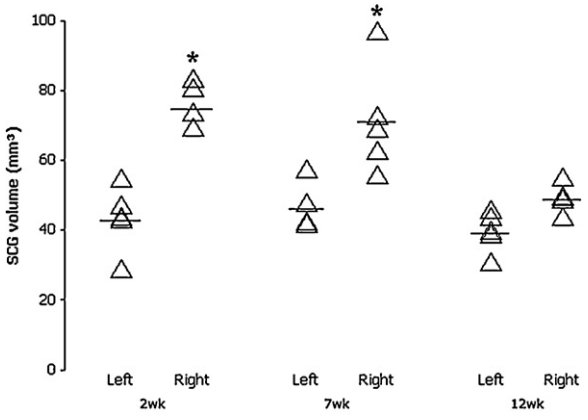

Fig. 3. SCG volume (V_{SCG}) of left (excised) and right (remaining) sheep SCG from groups 2, 7 and 12 weeks after surgery. Group differences were significant for the post-operative time effect ($p = 0.0012$* for group 2wk; 0.001* for group 7wk and 0.0001* for group 12wk) and there were significant ganglionectomy-induced differences (i.e. the right SCG tended to be bigger than the left at 2 and 7 weeks ($p = 0.004$* for group 2wk and 0.003* for group 7wk)). Triangles indicate individual values and horizontal bars show group means.

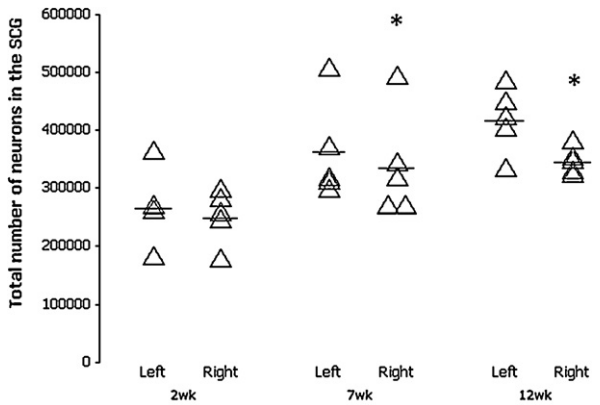

Fig. 4. Total number of neurons (N_{SCG}) in left (excised) and right (remaining) sheep SCG from groups 2, 7 and 12 weeks after surgery. Group differences were significant for the post-operative time effect ($p = 0.001$* for group 2wk; 0.001* for group 7wk and 0.0002* for group 12wk) and ganglionectomy-induced differences were significant only at 7 and 12 weeks ($p = 0.034$* for group 7wk and 0.018* for group 12wk). Triangles indicate individual values and horizontal bars show group means.

Please cite this article in press as: Fioretto, E.T., et al., Hypertrophy and neuron loss: structural changes in sheep SCG induced by unilateral sympathectomy. Int. J. Dev. Neurosci. (2011), doi:10.1016/j.ijdevneu.2011.02.002

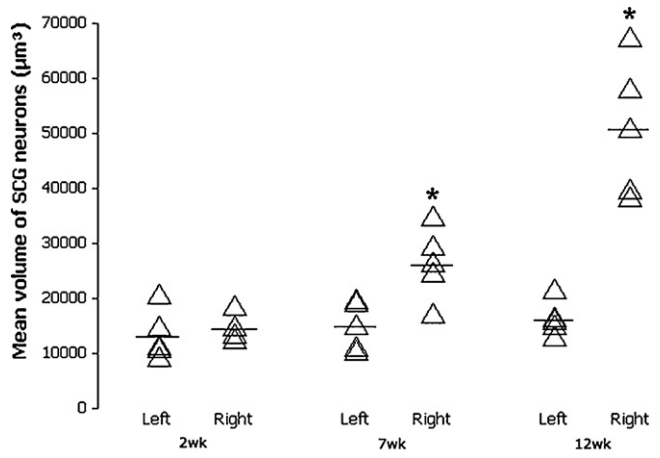

Fig. 5. Mean volume of left (excised) and right (remaining) sheep SCG neurons ($\bar{v}_{N\,SCG}$) from groups 2, 7 and 12 weeks after surgery. Group differences were significant for both the post-operative time ($p = 0.0003^*$ for group 2wk; 0.0002^* for group 7wk and 0.0001^* for group 12wk) and ganglionectomy-induced effects although the latter were significant only by 7 and 12 weeks ($p = 0.035^*$ for group 7wk and 0.001^* for group 12wk). Triangles indicate individual values and horizontal bars show group means. RL. Antonio Augusto Coppi.

3.3.3. Mean volume of SCG neuron, $\bar{v}_{N\,SCG}$

For group 2wk, the mean perikaryal volume of left and right SCG neurons was 13,040 μm^3 (0.34) and 14,390 μm^3 (0.16) respectively (Fig. 5). For group 7wk, the corresponding mean volumes were 14,710 μm^3 (0.29) and 26,150 μm^3 (0.25) and, for group 12wk, 16,000 μm^3 (0.20) and 50,470 μm^3 (0.24). There were significant effects of post-operative time and ganglionectomy-induced changes ($p < 0.001$ in both cases) and a significant interaction between them ($p < 0.001$). SCG neurons from animals in group 12wk tended to be bigger than neurons from groups 2wk and 7wk. Paired *t*-tests confirmed that ganglionectomy-induced differences in mean perikaryal volumes were not significant at 2 weeks but neurons were significantly greater in right SCGs at 7 weeks ($p = 0.035$) and 12 weeks ($p = 0.001$).

4. Discussion

In our sheep model of left unilateral ganglionectomy, our main findings were: (i) the right SCG tended to be bigger than the left but the lateral differences decreased with time after surgery (74% at 2 weeks, 55% at 7 weeks and no difference by 12 weeks), (ii) by 7 weeks after surgery, the right SCG harboured fewer neurons than the left SCG (no difference at 2 weeks, 6% fewer by 7 weeks and 17% fewer by 12 weeks) and (iii) by 7 weeks, right SCG neurons were also larger than those in the left and the magnitude of the difference increased markedly with time (no difference at 2 weeks, 77% by 7 weeks and 215% by 12 weeks).

4.1. Operative technique

Relative to the unilateral left SCG ganglionectomy described here, the original surgical approach described by Appleton and Waites (1957) was more invasive because it involved the partial resection of the zygomatic arch (midway between the eye and the base of the auricle) and thyroid cartilage. In the present study, a slightly modified surgical access (a ventro-lateral cervical approach) was undertaken in order to identify the left SCG and its surrounding structures. The surgical intervention was fairly successful, i.e. no casualties or complications were observed during the operative and post-operative periods.

4.2. Clinical findings

The main clinical findings during the post-operative period (high temperature of the face and ear, ptosis of the left upper eyelid, miosis and absence of sudoresis) are related to Horner's syndrome, which was milder than that described earlier in dogs (Kisch, 1991; Boydell, 1995; Bell et al., 2001). Symptoms persisted mostly for two weeks after surgery, with the exception of the ptosis of the left upper eyelid, which occurred until week 12.

The involvement of SCG in maintaining body temperature has been investigated in rats. Bilateral SCG ganglionectomy impaired the ability to induce a febrile response (Romeo et al., 2009) and rats subjected to SCG ganglionectomy barely survived in a cold environment beyond 48 h despite prior cold-adaptation for one month (Romeo et al., 1986). Taken together, these data suggest that SCG may be implicated in either physiological adaptation to thermal environment and febrile response or in producing a mild hypothermia (Romeo et al., 2009). Since bilateral SCG ganglionectomy impairs the ability to induce a febrile response, and SCG may be implicated in producing a mild hypothermia (Romeo et al., 2009), we hypothesise that the discrete rise in the face temperature (in the left side of the face) after surgery may be attributable to a compensatory thermal mechanism initiated by the right (remaining) SCG in response to the surgical procedure.

4.3. SCG structure

Irrespective of body side and week studied, all SCGs encapsulated the same structural arrangement which is in line with previous qualitative studies on the sympathetic ganglia of mammals including sheep, dogs, horses, cats and rabbits (Gabella et al., 1988; Ribeiro et al., 2002, 2004; Gagliardo et al., 2003; Ribeiro, 2006; Fioretto et al., 2007; Sasahara et al., 2003).

A notable finding in this study was the differential distribution of neurons between right and left SCGs, i.e. neurons were smaller, densely packed and homogeneously distributed in the excised left SCG, whereas neurons were bigger, unevenly distributed and separated by spaces mainly occupied by neuropil (neurites and glial cells) and by blood vessels and connective tissue in the non-operated right SCG. SCG neurons from some aged rodents, e.g. guinea pig and pacas, are also distributed non-uniformly and separated by non-neuronal tissue, especially connective tissue (Toscano et al., 2009; Abrahão et al., 2009; Melo et al., 2009).

4.4. Stereology

4.4.1. Ganglion volume

In all groups, the right (remaining) SCG appeared to be bigger than the left (excised) SCG. However, the right SCG hypertrophy decreased gradually after surgery and its volume was not significantly different from that of the left SCG by 12 weeks. In the present study, the increase in SCG volume could be explained by an increase in the combined volume of all perikarya and this occurred despite neuron loss. A number of previous studies have shown lesion-induced neuroplasticity resulting in increased innervation territory. By assessing the effects of a unilateral SCGx on rat tooth eruption, Ladizesky et al. (2001) reported a lower eruption rate of denervated incisors at the impeded eruption side, and a higher eruption rate of incisors at the unimpeded side. In addition, Ladizesky et al. (2000) assessed the effects of a unilateral SCGx on bone metabolism (bone mineral content and density) in the rat mandible. Their main results encapsulate an increase in the hemi-mandibular bone ipsilaterally to SCGx whereas a decrease in the hemi-mandibular bone was noticed contralateral to SCGx. Along similar lines, Wang et al. (1994) and Wang and Chiou (2004) documented the sympathetic cross-innervation of the Eustachian tube

Please cite this article in press as: Fioretto, E.T., et al., Hypertrophy and neuron loss: structural changes in sheep SCG induced by unilateral sympathectomy. Int. J. Dev. Neurosci. (2011), doi:10.1016/j.ijdevneu.2011.02.002

and of the tongue of rats subjected to unilateral SCGx respectively. By analogy, we hypothesise that the hypertrophy of the right SCG is the result of the increase in the size of its innervation territory, although the latter was not measured in the present study.

4.4.2. Total number of neurons

The right (remaining) SCG contained fewer neurons than the left (excised) SCG by 7 weeks post surgery and this depletion was greater by 12 weeks. The greater decrease in number of right SCG neurons in group 12wk was remarkable.

From the existing literature on sympathetic ganglionectomy, we found only one quantitative paper (Usui and Sakamaki, 1998). By employing histology and two-dimensional model-based morphometry, the authors reported on the effect of a unilateral superior cervical ganglionectomy on the contralateral ganglion of Sprague–Dawley rats. The aforementioned authors found no changes in the number of SCG neurons and this is in stark contrast to the neuron loss reported in our study. From our point of view, their data are nevertheless misleading, since Usui and Sakamaki (1998) did not estimate the total number of neurons (as we have performed) but rather the number of neuron profiles. (for more details, see Introduction.) We strongly contend that the 2D methodological approach could account for the discrepancy between the two sets of findings, rather than differences in animal species, i.e. rats vs sheep, or in postnatal development and survival time.

4.4.3. Neuron size

There is little information on the volumes of SCG neurons in sheep. Using a model-based morphometrical approach treating neurons as spheres, values were reported varying from 1600 μm^3 to 93,000 μm^3 (Gabella et al., 1988). These estimates are greater than our estimates (13,000–50,000 μm^3) which were obtained using a design-based stereological estimator, the nucleator. In other areas of quantitative morphology, the use of such stereological methods is likely to be beneficial in terms of estimation precision and bias, e.g. (Mühlfeld et al., 2010).

Except for 2 weeks post surgery, the neuron perikarya in right (remaining) SCGs were larger than those in the left (excised). The increases in neuron size were substantial: 78% (week 7) and 2-fold (week 12). Whilst using 2D model-based methods, Usui and Sakamaki (1998) also communicated neuron hypertrophy (in the remaining SCG neurons) induced by a unilateral superior cervical ganglionectomy in rats. The latter was interpreted as the result of a cross-innervation, viz, a nerve input from the contralateral territory previously innervated by the removed SCG. Despite the methodological differences (2D vs 3D), it seems that the increase in neuron size is a real event triggered by superior cervical ganglionectomy.

Neuron hypertrophy (Cabello et al., 2002; Gagliardo et al., 2005; Abrahão et al., 2009; Melo et al., 2009) or atrophy (Toscano et al., 2009) have been studied widely during ageing and, although age-related cell hypertrophy is usually considered to be an indication of cell degeneration or necrosis, a recent study has cast doubt on that proposition. Neuron hypertrophy could be a compensatory mechanism triggered by significant neuron loss. Therefore, the total amount of cell substance capable of producing essential transmitters would not be reduced to a critically low level as a result of ageing (Cabello et al., 2002; Sanchez et al., 2008). By the same token, another compensatory sympathetic growth (or ingrowth) from SCG into the hippocampus has been reported during degenerative disorders such as Alzheimer's disease. The rescue effect upon denervated hippocampal neurons consists in the fact that a peripheral adrenergic system can replace a central degenerated cholinergic system in terms of function in order to elicit neuroprotection (anti-apoptosis-like action) and synaptic plasticity (Masliah et al., 1991; Booze et al., 1993; Harrell et al., 2001, 2005a,b).

Hypertrophy has also been reported in pelvic ganglion neurons after rat urinary bladder outlet obstruction and contralateral pelvic ganglionectomy (Gabella et al., 1992; Gabella and Uvelius, 1993), and in the musculature of the obstructed rabbit urinary bladder (Sasahara et al., 2007).

4.5. Conclusions and remarks for future studies

We suggest that future studies may usefully focus on the functional and clinical consequences of the surgical ablation of SCG. Another interesting line of research enquiry would be the interaction between the SCGs and their innervation targets after ganglionectomy. Are there any grounds for believing in a ganglionectomy-induced SCG cross-innervation and neuroplasticity?

Acknowledgements

The Laboratory of Stochastic Stereology and Chemical Anatomy (LSSCA) is supported by São Paulo Research Foundation (FAPESP) (Application number 2004/15882-0). Authors thank Solange Mikail (DVM) for performing the thermographic analysis. JRN also thanks "Center for Stochastic Geometry and Advanced Bioimaging" supported by Villum Foundation.

References

Abrahão, L.M., Nyengaard, J.R., Sasahara, T.H., Gomes, S.P., Oliveira, F.R., Ladd, F.V., Ladd, A.A., Melo, M.P., Machado, M.R., Melo, S.R., Ribeiro, A.A., 2009. Asymmetric post-natal development of the superior cervical ganglion of pacas (*Agouti paca*). Int. J. Dev. Neurosci. 27, 37–45.

Andrews, T.J., 1996. Autonomic nervous system as a model of neuronal aging: the role of target tissues and neurotrophic factors. Microsc. Res. Tech. 35, 2–19.

Appleton, A.B., Waites, G.M.H., 1957. A surgical approach to the superior cervical ganglion and related structures in the sheep. J. Physiol. 135, 52–57.

Baddeley, A.J., Gundersen, H.J.G., Cruz-Orive, L.M., 1986. Estimation of surface area from vertical sections. J. Microsc. 142, 259–276.

Bell, R.L., Atweh, N., Ivy, M., Possenti, P., 2001. Traumatic and iatrogenic Horner syndrome: case reports and review of the literature. J. Trauma Inj. Infect. Crit Care 51, 400–404.

Booze, R.M., Mactutus, C.F., Gutman, C.R., Davis, J.N., 1993. Frequency analysis of catecholamine axonal morphology in human brain. II. Alzheimer's disease and hippocampal sympathetic ingrowth. J. Neurosci. 119, 110–118.

Boydell, P., 1995. Idiopathic Horner's syndrome in the Golden Retriever. J. Small Anim. Pract. 36, 382–384.

Braendgaard, H., Gundersen, H.J.G., 1986. The impact of recent stereological advances on quantitative studies of the nervous system. J. Neurosci. Meth. 18, 39–78.

Cabello, C.R., Thune, J.J., Pakkenberg, H., Pakkenberg, B., 2002. Ageing of substantia nigra in humans: cell loss may be compensated by hypertrophy. Neuropathol. Appl. Neurobiol. 28, 283–291.

Cruz-Orive, L.M., 1994. Toward a more objective biology. Neurobiol. Aging 15, 377–378.

Fioretto, E.T., Abreu, R.N., Castro, M.F., Guidi, W.L., Ribeiro, A.A., 2007. Macro- and microstructure of the superior cervical ganglion in dogs, cats and horses during maturation. Cell Tiss. Organ. 186, 129–140.

Gabella, G., Trigg, P., Mcphail, H., 1988. Quantitative cytology of ganglion neurons and satellite glial cells in the superior cervical ganglion of the sheep. Relationship with ganglion neuron size. J. Neurocytol. 17, 753–769.

Gabella, G., Berggren, T., Uvelius, B., 1992. Hypertrophy and reversal of hypertrophy in rat pelvic ganglion neurons. J. Neurocytol. 21, 649–662.

Gabella, G., Uvelius, B., 1993. Effect of decentralization or contralateral ganglionectomy on obstruction-induced hypertrophy of rat urinary bladder muscle and pelvic ganglion. J. Neurocytol. 22, 827–834.

Gagliardo, K.M., Guidi, W.L., Da Silva, R.A., Ribeiro, A.A., 2003. Macro and microstructural organization of the dog's caudal mesenteric ganglion complex (*Canis familiaris*). Anat. Histol. Embryol. 32, 236–243.

Gagliardo, K.M., Carvalho, B.J.C., Souza, R.R., Ribeiro, A.A., 2005. Postnatal-related changes in the size and total number of neurons in the caudal mesenteric ganglion of dogs: total number of neurons can be predicted from body weight and ganglion volume. Anat. Rec. 286, 917–929.

Gundersen, H.J.G., 1977. Notes of the estimation of the numerical density of arbitrary profiles: the edge effect. J. Microsc. 111, 219–223.

Gundersen, H.J.G., 1986. Stereology of arbitrary particles. A review of unbiased number and size estimators and the presentation of some new ones, in memory of William R. Thompson. J. Microsc. 143, 3–45.

Gundersen, H.J.G., Jensen, E.B., 1987. The efficiency of systematic sampling in stereology and its prediction. J. Microsc. 147, 229–263.

Please cite this article in press as: Fioretto, E.T., et al., Hypertrophy and neuron loss: structural changes in sheep SCG induced by unilateral sympathectomy. Int. J. Dev. Neurosci. (2011), doi:10.1016/j.ijdevneu.2011.02.002

Gundersen, H.J.G., 1988. The nucleator. J. Microsc. 151, 3–21.
Gundersen, H.J.G., Jensen, E.B., Kiêu, K., Nielsen, J., 1999. The efficiency of systematic sampling in stereology: reconsidered. J. Microsc. 193, 199–211.
Harrell, L.E., Parsons, D., Kolasa, K., 2001. Hippocampal sympathetic ingrowth occurs following 192-IgG-saporin administration. Brain Res. 911, 158–162.
Harrell, L.E., Parsons, D.S., Kolasa, K., 2005a. The effect of central cholinergic and noradrenergic denervation on hippocampal sympathetic ingrowth and apoptosis-like reactivity in the rat. Brain Res. 1033, 68–77.
Harrell, L.E., Parsons, D.S., Kolasa, T.K., 2005b. Pro- and anti-apoptotic evidence for cholinergic denervation and hippocampal sympathetic ingrowth in rat dorsal hippocampus. Exp. Neurol. 194, 182–190.
Hunziker, E.B., Cruz-Orive, L.M., 1986. Consistent and efficient delineation of reference spaces for light microscopical stereology using a laser microbeam system. J. Microsc. 142, 95–99.
Karasek, M., Zielinska, A., Marek, K., Swietoslawski, J., 2002. Effect of superior cervical ganglionectomy on the ultrastructure of pinealocytes in the Djungarian hamster (*Phodopus sungorus*): quantitative study. Neuroendocrinol. Lett. 23, 443–446.
Kim, Y., Hamada, N., Takahashi, Y., Sasaguri, K., Tsukinoki, K., Onozuka, M., Sato, S., 2009. Cervical sympathectomy causes alveolar bone loss in an experimental rat model. J. Periodont. Res. 44, 695–703.
Kisch, B., 1991. Horner's syndrome, an American discovery. Bull Hist. Med. 25, 284–288.
Ladizesky, M.G., Cutrera, R.A., Boggio, V., Mautalen, C., Cardinali, D.P., 2000. Effect of unilateral superior cervical ganglionectomy on bone mineral content and density of rat's mandible. J. Auton. Nerv. Syst. 78, 113–116.
Ladizesky, M.G., Lama, M.A., Cutrera, R.A., Boggio, V., Giglio, M.J., Cardinali, D.P., 2001. Effect of unilateral superior cervical ganglionectomy on mandibular incisor eruption rate in rats. Auton. Neurosci. 93, 65–70.
Masliah, E., Mallory, M., Hansen, L.A., Alford, M., Albright, T., De Teresa, R., Terry, R., Baudier, J., Saitoh, T., 1991. Patterns of aberrant sprouting in Alzheimer's disease. Neuron 6, 729–739.
Mayhew, T.M., 1991. The accurate prediction of Purkinje cell number from cerebellar weight can be achieved with the fractionator. J. Comp. Neurol. 308, 162–168.
Mayhew, T.M., 2008. Taking tissue samples from the placenta: an illustration of principles and strategies. Placenta 29, 1–14.
Melo, S.R., Nyengaard, J.R., Oliveira, F.R., Ladd, F.V., Abrahão, L.M., Machado, M.R., Sasahara, T.H., Melo, M.P., Ribeiro, A.A., 2009. The developing left superior cervical ganglion of pacas (*Agouti paca*). Anat. Rec. 292, 966–975.
Mühlfeld, C., Nyengaard, J.R., Mayhew, T.M., 2010. A review of state-of-the-art stereology for better quantitative 3D morphology in cardiac research. Cardiovasc. Pathol. 19, 65–82.
Polkowska, J., Wójcik-Gladysz, A., Wańkowska, M., Bruneau, G., Tillet, Y., 2008. Prepubertal changes in the synthesis, storage and release of somatostatin in the hypothalamus of female lambs: a morphofunctional study. J. Chem. Neuroanat. 36, 53–58.
Purohit, R.C., McCoy, M.D., Bergfeld, W.A., 1980. Thermographic diagnosis of Horner's syndrome in the horse. Am. J. Vet. Res. 41, 1180–1182.
Raju, B., Hultström, M., Haug, S.R., Ibrahim, S.O., Heyeraas, K.J., 2009. Sympathectomy suppresses tumor growth and alters gene-expression profiles in rat tongue cancer. Eur. J. Oral Sci. 117, 351–361.
Ribeiro, A.A., Elias, C.F., Liberti, E.A., Guidi, W.L., De Souza, R.R., 2002. Structure and ultrastructure of the celiac mesenteric ganglion complex in the domestic dog (*Canis familiaris*). Anat. Histol. Embryol. 31, 344–349.
Ribeiro, A.A., Davis, C., Gabella, G., 2004. Estimate of size and total number of neurons in superior cervical ganglion of rat, capybara and horse. Anat. Embryol. 208, 367–380.
Ribeiro, A.A., 2006. Size and number of binucleate and mononucleate superior cervical ganglion neurons in young capybaras. Anat. Embryol. 211, 607–617.
Romeo, H.E., Cardinali, D.P., Boado, R.J., Zaninovich, A.A., 1986. Effect of superior cervical ganglionectomy on thyroidectomy-induced increase of serum TSH and on survival of rat in a cold environment. Neuroendocrinol. Lett. 8, 269–272.
Romeo, H.E., Tio, D.L., Taylor, A.N., 2009. Effects of superior cervical ganglionectomy on body temperature and on the lipopolysaccharide-induced febrile response in rats. J. Neuroimmunol. 209, 81–86.
Sanchez, H.L., Silva, L.B., Portiansky, E.L., Herenu, C.B., Goya, R.G., Zuccolilli, G.O., 2008. Dopaminergic mesencephalic systems and behavioral performance in very old rats. Neuroscience 154, 1598–1606.
Sasahara, T.H., De Souza, R.R., Machado, M.R., Da Silva, R.A., Guidi, W.L., Ribeiro, A.A., 2003. Macro- and microstructural organization of the rabbit's celiac-mesenteric ganglion complex (*Oryctolagus cuniculus*). Ann. Anat. 185, 441–448.
Sasahara, T.H.C., Mayhew, T.M., Rahal, S.C., Fioretto, E.T., Balieiro, J.C., Ribeiro, A.A., 2007. Partial urethral obstruction of rabbit urinary bladder. Stereological evidence that the increase in muscle content is mostly driven by changes in number, rather than size, of smooth muscle cells. J. Anat. 210, 449–459.
Steele, C., Fioretto, E.T., Sasahara, T.H., Guidi, W.L., de Lima, A.R., Ribeiro, A.A., Loesch, A., 2006. On the atrophy of the internal carotid artery in capybara. Cell Tissue Res. 326, 737–748.
Tandrup, T., 1993. A method for unbiased and efficient estimation of number and mean volume of specified neuron subtypes in rat dorsal root ganglion. J. Comp. Neurol. 329, 269–276.
Tandrup, T., Braendgaard, H., 1994. Number and volume of rat dorsal root ganglion cells in acrylamide intoxication. J. Neurocytol. 23, 242–248.
Toscano, C.P., Melo, M.P., Matera, J.M., Loesch, A., Ribeiro, A.A., 2009. The developing and restructuring superior cervical ganglion of guinea pigs (*Cavia porcellus var. albinus*). Int. J. Dev. Neurosci. 27, 329–336.
Usui, T., Sakamaki, Y., 1998. Effect of unilateral superior cervical sympathetic ganglionectomy on the contralateral ganglion in rat. Masui 47, 1183–1186.
Wang, H.W., Lin, J.K., Wang, J.Y., 1994. Sympathetic innervation of the eustachian tube in rats. Eur. Arch. Otorhinolaryngol. 251, 283–286.
Wang, H.W., Chiou, W.Y., 2004. Sympathetic innervation of the tongue in rats. ORL J. Otorhinolaryngol. Relat. Spec. 66, 16–20.
Wańkowska, M., Polkowska, J., 2006. The postnatal ontogeny of gonadotroph cells in the female sheep. Developmental patterns of synthesis, storage and release of gonadotrophic hormones. J. Chem. Neuroanat. 31, 130–138.
Wańkowska, M., Misztal, T., Romanowicz, K., Wójcik-Gladysz, A., Polkowska, J., 2008a. The intrapituitary endocrine events during maturation and timing of puberty in the female sheep. Anim. Reprod. Sci. 105, 258–271.
Wańkowska, M., Romanowicz, K., Polkowska, J., 2008b. The neuroendocrine events during the ovine growth-promoted maturation: the developmental importance of hypophysiotrophic action of somatostatin in ewes. Anim. Reprod. Sci. 109, 146–160.
Weibel, E.R., 1979. Stereological Methods. Vol. 1. Practical Methods for Biological Morphometry, 21. Academic Press, London, p. 415.
Zhan, G.L., Ohia, S.E., Camras, C.B., Ohia, E.O., Wang, Y.L., 1999. Superior cervical ganglionectomy-induced lowering of intraocular pressure in rabbits: role of prostaglandins and neuropeptide Y. Gen. Pharmacol. 32, 189–194.

Please cite this article in press as: Fioretto, E.T., et al., Hypertrophy and neuron loss: structural changes in sheep SCG induced by unilateral sympathectomy. Int. J. Dev. Neurosci. (2011), doi:10.1016/j.ijdevneu.2011.02.002